Reaction Rates and Energy Spectra for Nuclear Reactions in High Energy Plasmas

G. Lehner

IPP 1/101 September 1969

INSTITUT FÜR PLASMAPHYSIK

GARCHING BEI MÜNCHEN

INSTITUT FÜR PLASMAPHYSIK

GARCHING BEI MÜNCHEN

Reaction Rates and Energy Spectra for Nuclear Reactions in High Energy Plasmas

G. Lehner

IPP 1/101 September 1969

Die nachstehende Arbeit wurde im Rahmen des Vertrages zwischen dem Institut für Plasmaphysik GmbH und der Europäischen Atomgemeinschaft über die Zusammenarbeit auf dem Gebiete der Plasmaphysik durchgeführt.

IPP 1/101

G. Lehner

Reaction Rates and Energy Spectra for Nucear Reactions in High Energy Plasmas.

September 1969 (in English)

Abstract

Total reaction rates and energy spectra of the generated particles are discussed for fusion reactions in high energy plasmas. Examples, discussed in some detail, concern elliptic and mono-energetic velocity distributions of the plasma. One obtains energy spectra with very typical shapes which should be useful for diagnostic purposes. This is true in particular, of reactions between different particles such as the d - t reaction.

1) Introduction

Measurements of both the total reaction rates and of the energy spectra of the particles generated by nuclear reactions in hot plamas may be an interesting source of information on the plasma. A rather detailed discussion concerning the d(d,n) He^3 reaction has been given in /1/. Both d-d reactions are exceptions among fusion reactions between light nuclei since they are highly anisotropic. This fact offers another possibility of gaining information on the plasma by measuring a possible anisotropy of the emitted neutron flux (or of the emitted He^3 flux, which however, cannot be measured as easily). Some details concerning this anisotropy can be found in /1/. The effect has also been demonstrated experimentally, and its usefulness as a diagnostic tool has been shown /2,3/. In the present report, however, we consider isotropic reactions only. We do not specify at all the reaction considered, and we discuss the general features of reaction rates and energy spectra for plasmas with several typical velocity distributions of the ions. The most interesting example of such a reaction, besides the d-d reaction, is the d-t reaction, which will be dealt with in another report /4/.

We consider a reaction of the following type:

$$A + B \longrightarrow C + D + Q \qquad (1)$$

Q is the reaction energy. The masses of the particles are m_A, m_B, m_C, m_D. The reaction is assumed to be isotropic (in the centre-of-mass system), and its total cross section is $\sigma(g)$, where g is the relative velocity. We shall calculate the reaction rates for given velocity distributions of the particles A and B and the energy spectra of the generated particles C and D.

As in /1/, we shall consider various elliptic and monoenergetic distributions for A and B as typical examples. We shall see that the spectra may have very typical shapes, especially for reactions between two different types of particles such as d and t.

The plasma is supposed to contain particles A and B with densities n_A and n_B and velocity distribution functions f_A and f_B, which

are normalized to unity:

$$\int f_{A,B}(\vec{u})\, d^3u = 1 \tag{2}$$

We consider a pair of particles with velocities $\vec{u}_A$ and $\vec{u}_B$, relative velocity $\vec{g}$ and centre-of-mass velocity $\vec{s}$:

$$\vec{s} = \frac{m_A \vec{u}_A + m_B \vec{u}_B}{m_A + m_B} \tag{3}$$

$$\vec{g} = \vec{u}_A - \vec{u}_B \tag{4}$$

or

$$\vec{u}_A = \vec{s} + \frac{\mu}{m_A}\vec{g} \tag{5}$$

$$\vec{u}_B = \vec{s} - \frac{\mu}{m_B}\vec{g} \tag{6}$$

where

$$\mu = \frac{m_A m_B}{m_A + m_B} \tag{7}$$

is the reduced mass. The reaction rate is then

$$R = n_A n_B \iint f_A\left(\vec{s} + \frac{\mu}{m_A}\vec{g}\right) f_B\left(\vec{s} - \frac{\mu}{m_B}\vec{g}\right) g\,\sigma(g)\, d^3g\, d^3s$$

$$= n_A n_B \langle \sigma g \rangle \tag{8}$$

Sometimes it proves useful to describe the plasma by elliptic distributions as

$$f = \frac{\beta_\perp \beta_\parallel^{1/2}}{\pi^{3/2}} \exp\left(-\beta_\perp u_\perp^2 - \beta_\parallel u_\parallel^2\right) \tag{9}$$

where

$$\beta_\perp = \frac{m}{2kT_\perp} \quad , \quad \beta_\parallel = \frac{m}{2kT_\parallel} \tag{10}$$

We assume that both kinds of particles, A and B, have the same perpendicular temperature $T_\perp$ and the same parallel temperature $T_\parallel$. The product $f_A \cdot f_B$, which is needed for evaluating (8) may be written as follows:

$$f_A(\vec{u}_A) f_B(\vec{u}_B) = S(\vec{s})\, G(\vec{g}) \tag{11}$$

where both S and G are also elliptic and normalised to unity,

$$S(\vec{s}) = \frac{\beta_{\perp M} \beta_{\parallel M}^{1/2}}{\pi^{3/2}} \exp\left(-\beta_{\perp M} s_\perp^2 - \beta_{\parallel M} s_\parallel^2\right) \tag{12}$$

$$G(\vec{g}) = \frac{\beta_{\perp\mu} \beta_{\parallel\mu}}{\pi^{3/2}} \exp\left(-\beta_{\perp\mu} g_\perp^2 - \beta_{\parallel\mu} g_\parallel^2\right) \tag{13}$$

M is the total mass,

$$M = m_A + m_B \tag{14}$$

and

$$\beta_{\perp M} = \frac{M}{2kT_\perp} \quad , \quad \beta_{\parallel M} = \frac{M}{2kT_\parallel} \tag{15}$$

$$\beta_{\perp\mu} = \frac{\mu}{2kT_\perp} \quad , \quad \beta_{\parallel\mu} = \frac{\mu}{2kT_\parallel} \tag{16}$$

We shall also use three-dimensional monoenergetic distributions like

$$f(\vec{u}) = \frac{\delta(u^2 - u_0^2)}{2\pi u_0} \tag{17}$$

and two-dimensional monoenergetic distributions like

$$f(\vec{u}) = \frac{\delta(u_\perp^2 - u_0^2)\,\delta(u_\parallel)}{\pi} \qquad (18)$$

In this case $\vec{s}$ and $\vec{g}$ do not separate as for elliptic distributions. It is, however, useful to transform the product $f_A \cdot f_B$ in the following manner:

$$f_A(\vec{u}_A) f_B(\vec{u}_B) = \frac{1}{4\pi^2 u_{0A} u_{0B}} \delta(u^2 - u_{0A}^2)\,\delta(u^2 - u_{0B}^2)$$
$$= \frac{1}{4\pi^2 u_{0A} u_{0B}} \delta\left(s^2 + \frac{\mu^2}{m_A m_B} g^2 - \frac{\mu}{m_A} u_{0B}^2 - \frac{\mu}{m_B} u_{0A}^2\right) \qquad (19)$$
$$\cdot \delta\left(\mu\left(\frac{1}{m_B} - \frac{1}{m_A}\right) g^2 + u_{0A}^2 - u_{0B}^2 - 2\vec{s}\cdot\vec{g}\right)$$

in the three-dimensional case and

$$f_A(\vec{u}_A) f_B(\vec{u}_B) = \frac{1}{\pi^2} \delta\left(s_\perp^2 + \frac{\mu^2}{m_A m_B} g_\perp^2 - \frac{\mu}{m_A} u_{0B}^2 - \frac{\mu}{m_B} u_{0A}^2\right) \cdot$$
$$\cdot \delta\left(\mu\left(\frac{1}{m_B} - \frac{1}{m_A}\right) g_\perp^2 + u_{0A}^2 - u_{0B}^2 - 2\vec{s}_\perp \cdot \vec{g}_\perp\right) \delta(s_\parallel)\,\delta(g_\parallel) \qquad (20)$$

in the two-dimensional case.

2. Reaction Rates

For elliptic distributions we get from equations (8), (11), (12), (13) after integration with respect to $\vec{s}$

$$\langle \sigma g \rangle = \frac{\beta_{\perp\mu}\beta_{\parallel\mu}^{1/2}}{\pi^{3/2}} \int \exp\left(-\beta_{\perp\mu} g_\perp^2 - \beta_{\parallel\mu} g_\parallel^2\right) g\,\sigma(g)\,d^3g \qquad (21)$$

Thus, for an isotropic Maxwellian

$$\langle \sigma g \rangle_{3maxw} = 4\pi \left(\frac{\mu}{2\pi kT}\right)^{3/2} \int_0^\infty exp\left(-\frac{\mu g^2}{2kT}\right) g^3 \sigma(g)\, dg \qquad (22)$$

while for a two-dimensional Maxwellian $\left(T_{\parallel} \Rightarrow 0, \beta_{\parallel} \Rightarrow \infty\right)$

$$\langle \sigma g \rangle_{2maxw} = \frac{\mu}{kT_\perp} \int_0^\infty exp\left(-\frac{\mu g^2}{2kT_\perp}\right) g^2 \sigma(g)\, dg \qquad (23)$$

and for a one-dimensional Maxwellian $\left(T_\perp \Rightarrow 0, \beta_\perp \Rightarrow \infty\right)$

$$\langle \sigma g \rangle_{1maxw} = \left(\frac{2\mu}{\pi kT_{\parallel}}\right)^{1/2} \int_0^\infty exp\left(-\frac{\mu g^2}{2kT_{\parallel}}\right) g\, \sigma(g)\, dg \qquad (24)$$

The last two equations are most easily obtained by using

$$\lim_{\beta \to \infty} \sqrt{\frac{\beta}{\pi}}\, exp\left(-\beta x^2\right) = \delta(x) \qquad (25)$$

In the general elliptic case equation (21) may be rewritten as

$$\begin{aligned} \langle \sigma g \rangle &= \frac{2\beta_{\perp\mu}\beta_{\parallel\mu}^{1/2}}{\sqrt{\beta_{\parallel\mu} - \beta_{\perp\mu}}} \int_0^\infty exp\left(-g^2\beta_{\perp\mu}\right) erf\left(g\sqrt{\beta_{\parallel\mu} - \beta_{\perp\mu}}\right) g^2 \sigma(g)\, dg \\ &= \frac{2\beta_{\perp\mu}\beta_{\parallel\mu}^{1/2}}{\sqrt{\beta_{\perp\mu} - \beta_{\parallel\mu}}} \int_0^\infty exp\left(-g^2\beta_{\perp\mu}\right) erfi\left(g\sqrt{\beta_{\perp\mu} - \beta_{\parallel\mu}}\right) g^2 \sigma(g)\, dg \end{aligned} \qquad (26)$$

where

$$erf(x) = \frac{2}{\sqrt{\pi}} \int_0^x e^{-z^2} dz \qquad (27)$$

and

$$erfi(x) = -\, i\, erf(ix) \qquad (28)$$

For a three-dimensional monoenergetic plasma equations (8), (17), and (19) give

$$\langle \sigma g \rangle_{3\,mono} = \frac{1}{2 u_{0A} u_{0B}} \int_{|u_{0A}-u_{0B}|}^{u_{0A}+u_{0B}} \sigma(g)\, g^2\, dg \qquad (29)$$

In a similar manner, using equation (20) instead of equation (19), we obtain the reaction rate for a two-dimensional monoenergetic plasma

$$\langle \sigma g \rangle_{2\,mono} = \frac{2}{\pi} \int_{|u_{0A}-u_{0B}|}^{u_{0A}+u_{0B}} \frac{g^2 \sigma(g)\, dg}{\sqrt{g^2-(u_{0A}-u_{0B})^2}\sqrt{(u_{0A}+u_{0B})^2-g^2}} \qquad (30)$$

The integrand diverges both at the lower and at the upper limit of the integral. The integral itself is, of course, finite. The special case $u_0 = u_{0A} = u_{0B}$ brings us back to the simpler result

$$\langle \sigma g \rangle_{2\,mono} = \frac{1}{\pi} \int_{0}^{2u_0} \frac{g\,\sigma(g)\, dg}{\sqrt{u_0^2 - \frac{g^2}{4}}} \qquad (31)$$

which is used in /1/.

We may, for completeness, add the trivial one-dimensional monoenergetic case, for which

$$\langle \sigma g \rangle_{1\,mono} = \frac{u_{0A}+u_{0B}}{2}\, \sigma(u_{0A}+u_{0B}) \qquad (32)$$

Another report /4/ will contain numerical results of the reaction rates for several distribution functions concerning the d-t reaction.

3. Energy spectra

Let us now discuss the more involved problem of the energy spectra. As Q is the reaction energy the total energy available to both particles generated by the reaction is, in the centre-of-mass system,

$$Q + \frac{m_A}{2}\left(\vec{u}_A - \vec{s}\right)^2 + \frac{m_B}{2}\left(\vec{u}_B - \vec{s}\right)^2 = Q + \frac{\mu}{2} g^2 \qquad (33)$$

The fraction of energy given to the particle C, for instance, is

$$\hat{E}_c = \frac{m_c w_c^2}{2} = \frac{m_D}{m_c + m_D}\left(Q + \frac{\mu}{2} g^2\right) \qquad (34)$$

or

$$w_c(g) = \sqrt{\frac{2 m_D}{m_c (m_c + m_D)}\left(Q + \frac{\mu}{2} g^2\right)} \qquad (35)$$

where w_c, the velocity of particle C in the centre-of-mass system, is a function of g.

$$\vec{v} = \vec{w} + \vec{s} \qquad (36)$$

is its velocity in the laboratory system of reference. If E_c is its energy in the laboratory system, the energy spectrum may thus be written as

$$\frac{d^2 R}{d\Omega\, dE_c} = \frac{n_A n_B v}{2\pi m_c} \iint f_A\left(\vec{v} - \vec{w} + \frac{\mu}{m_A}\vec{g}\right) f_B\left(\vec{v} - \vec{w} - \frac{\mu}{m_B}\vec{g}\right) \cdot \frac{g\,\sigma(g)}{w}\, \delta\left(w^2 - w_c^2\right) d^3 g\, d^3 w \qquad (37)$$

To obtain this we rewrite equation (8) in the following form:

$$R = n_A n_B \iiint f_A\left(\vec{s} + \frac{\mu}{m_A}\vec{g}\right) f_B\left(\vec{s} - \frac{\mu}{m_B}\vec{g}\right) g\,\sigma(g) \cdot$$
$$\cdot \frac{\delta(w^2 - w_c^2)}{2\pi w}\, d^3w\, d^3g\, d^3s$$
$$= n_A n_B \iiint f_A\left(\vec{v} - \vec{w} + \frac{\mu}{m_A}\vec{g}\right) f_B\left(\vec{v} - \vec{w} - \frac{\mu}{m_B}\vec{g}\right) g\,\sigma(g) \cdot$$
$$\cdot \frac{\delta(w^2 - w_c^2)}{2\pi w}\, d^3w\, d^3g\, d^3v$$

and this leads to equation (37) because

$$d^3v = d\Omega\, dv\, v^2 = \frac{d\Omega\, dE_c\, v}{m_c}$$

where $d\Omega$ is the solid angle differential in the laboratory system.

We shall now give the results obtained by using several distribution functions in (37) without going into the details of derivation because these are, at least for some of the cases, rather unwieldy and of little interest.

3a. Three-dimensional isotropic Maxwellian

In this case we have

$$\frac{dR}{dE_c} = \frac{2 n_A n_B \mu \sqrt{M\mu}}{\pi m_c (kT)^2} \int_0^\infty \exp\left[-\beta_M\left(v^2 + w_c^2\right) - \beta_\mu g^2\right] \cdot$$
$$\cdot \sinh\left(2\beta_M v w_c\right) \frac{g^3 \sigma(g)}{w_c(g)}\, dg \qquad (38)$$

i.e. we are left with only one integration which cannot be performed analytically. If, however, as we can assume for all actual plasmas,

$$kT \ll Q \qquad (39)$$

the spectrum (38) may be approximated by

$$\frac{dR}{dE_c} \approx \frac{n_A n_B}{m_c v_0} \left(\frac{\beta_M}{\pi}\right)^{1/2} \langle \sigma g \rangle_{3maxw} \exp\left[-\beta_M (v - v_0)^2\right] \qquad (40)$$

where

$$v_0 = \sqrt{\frac{2 m_D}{m_c (m_c + m_D)} Q} \qquad (41)$$

is the velocity particle C would have after a reaction between two particles at rest in the centre-of-mass system. We see that the energy spectrum is Gaussian with a half-width

$$\Delta E_c \approx 4 \sqrt{\frac{m_c m_D \ln 2}{(m_A + m_B)(m_c + m_D)} Q kT} \qquad (42)$$

or

$$\Delta E_c \approx \frac{4 \sqrt{m_c m_D \ln 2 \, Q kT}}{m_A + m_B} \qquad (43)$$

because

$$m_A + m_B \approx m_c + m_D \qquad (44)$$

The half-width is symmetric with respect to particles C and D , i.e. it is the same for both particles:

$$\Delta E_c = \Delta E_D = \Delta E \qquad (45)$$

Table 1 below gives ΔE for some of the most important fusion reactions.

TABLE 1:

ΔE for several fusion reactions

reaction	Q (MeV)	E (keV) (kT in keV)
d(d,n) He^3	3.27	$82.5\sqrt{kT}$
d(d,p) H^3	4.04	$92\sqrt{kT}$
d(t,n)He^4	17.58	$177\sqrt{kT}$
d(He^3,p)He^4	18.34	$181\sqrt{kT}$

3b. Two-dimensional Maxwellian

The spectrum is given by

$$\frac{d^2R}{d\Omega\, dE_c} = \frac{n_A n_B M \mu\, v \pi}{m_c (2\pi k T_\perp)^2} \cdot \int_{g_{min}}^{\infty} \exp\left[-\beta_{\perp M}\left(v_\perp^2 + w_c^2 - v_\parallel^2\right) - \beta_{\perp\mu} g^2\right] \cdot$$

$$\cdot I_0\left(2\beta_{\perp M} v_\perp \sqrt{w_c^2 - v_\parallel^2}\right) \frac{g^2 S(g)}{w_c}\, dg \qquad (46)$$

I_0 is the modified Bessel function. The integration is not to be extended over all values of g. Because $S_\parallel = 0$ for a two-dimensional distribution

$$v_\parallel^2 < w_c^2 \qquad (47)$$

The argument of I_0 is thus real. From (47) we get

$$Q + \frac{\mu}{2} g^2 > \frac{m_c (m_c + m_D)}{2 m_D} v_\parallel^2 \qquad (48)$$

and

$$g^2 > g_{min}^2 = \begin{cases} \frac{2}{\mu}\left[\frac{m_c(m_c+m_D)}{2m_D} v_{\parallel}^2 - Q\right] & \text{if positive} \\ 0 & \text{if the above expression is negative.} \end{cases} \qquad (49)$$

For $kT \ll Q$ I_0 can be approximated by an exponential function, and we get

$$\frac{d^2R}{d\Omega dE_c} \sim \exp\left[-\beta_\perp m\left(v_\perp - \sqrt{w_c^2 - v_\parallel^2}\right)^2\right] \qquad (50)$$

i.e. a Gaussian spectrum with the half-width

$$\Delta E_c \approx \frac{4\sqrt{m_c m_D \ln 2\, Q\, kT}}{m_A + m_B} \sin\alpha \qquad (51)$$

where α is the angle between the direction of observation and the axis. Thus for the perpendicular direction we get the same result as in the three-dimensional case, and towards the axis the spectrum contracts as $\sin\alpha$. This is, however, not true for very small angles α . Our approximation is correct only if the argument of I_0 is much larger than one, i.e. if

$$\sin\alpha \gg \sqrt{\frac{kT}{Q}} \qquad (52)$$

For angles of that order of magnitude or smaller the spectrum is no larger Gaussian and is now highly asymmetric.

The spectrum (46) may be integrated to give the reaction rate (23) . This can be done by using the relation

$$\int_0^\infty \exp\left(-p^2x^2\right) J_0(ax)\, x\, dx = \int_0^\infty \exp\left(-p^2x^2\right) I_0(iax)\, x\, dx = \frac{1}{2p^2}\exp\left(-\frac{a^2}{4p^2}\right) \qquad (53)$$

which allows integration with respect to $v_\perp$. Integrating with respect to $v_\parallel$ one has to take into account that

$$-w_c \le v_\parallel \le w_c \,.$$

3c. One-dimensional Maxwellian

In this case

$$\frac{d^2R}{d\Omega dE_c} = \frac{n_A n_B v \sqrt{M\mu}}{4\pi^2 m_c kT_{\parallel}} \int_{g_{min}}^{\infty} exp\left(-\beta_{\parallel M} g^2\right) g\sigma(g) \cdot$$

$$\cdot \frac{exp\left[-\beta_{\parallel M}\left(v_{\parallel} + \sqrt{w_c^2 - v_{\perp}^2}\right)^2\right] + exp\left[-\beta_{\parallel M}\left(v_{\parallel} - \sqrt{w_c^2 - v_{\perp}^2}\right)^2\right]}{w_c \sqrt{w_c^2 - v_{\perp}^2}} dg \qquad (54)$$

Integration with respect to $\vec{v}$ yields the total reaction rate as given by equation (24). For $kT \ll Q$ we can again approximate the spectrum by

$$\frac{d^2R}{d\Omega dE_c} \sim exp\left[-\beta_{\parallel M}\left(v_{\parallel} - \sqrt{w_c^2 - v_{\perp}^2}\right)^2\right] \qquad (55)$$

and the half-width is now

$$\Delta E_c \simeq \frac{4\sqrt{m_c m_D Q^2 Q kT}}{m_A + m_B} \cos\alpha \qquad (56)$$

Thus for observation along the axis we again have the values of $\Delta E_c = \Delta E$ in Table 1. For larger angles the spectrum shrinks as $\cos\alpha$, where α should not be very close to $\pi/2$ i.e. $\cos\alpha$ has to obey

$$\cos\alpha \gg \sqrt{\frac{kT}{Q}} \qquad (57)$$

g_{min} is now defined by the fact that $v_{\perp}^2 < w_c^2$ i.e. we have

$$g^2 > g_{min} = \begin{cases} \frac{2}{\mu}\left[\frac{m_c(m_c+m_D)}{2m_D} v_{\perp}^2 - Q\right] & \text{if positive} \\ 0 & \text{if the above expression is negative.} \end{cases} \qquad (58)$$

3d. Three-dimensional monoenergetic Velocity distributions

In this case integration can be shown to give

$$\frac{dR}{dE_z} = \frac{n_A n_B}{4 m_C u_{0A} u_{0B}} \int_R \frac{g^2 \sigma(g)\, dg}{w_c(g) \sqrt{\frac{\mu}{m_A} u_{0B}^2 + \frac{\mu}{m_B} u_{0A}^2 - \frac{\mu^2}{m_A m_B} g^2}} \qquad (59)$$

The integrand does not depend at all on v . This does not mean, however, that we get a constant spectrum because the region R of integration depends on v . It is the region R which we have to discuss now. The root in the denominator of the integrand represents the velocity of the centre-of-mass (see equation (19)). If g is given, the maximum and minimum values which v can have are

$$v_\pm = w_c \pm s = \sqrt{\frac{2 m_D}{(m_C + m_D) m_C} \left(Q + \frac{\mu}{2} g^2\right)} \pm \sqrt{\frac{\mu}{m_A} u_{0B}^2 + \frac{\mu}{m_B} u_{0A}^2 - \frac{\mu^2}{m_A m_B} g^2} \qquad (60)$$

This may be written as

$$v_\pm = \sqrt{a + b g^2} \pm \sqrt{c - d g^2} \qquad (61)$$

where a,b,c,d are positive constants:

$$\left.\begin{aligned} a &= \frac{2 m_D}{(m_C + m_D) m_C} Q = v_0^2 \\ b &= \frac{m_D \mu}{m_C (m_C + m_D)} \\ c &= \frac{m_B u_{0B}^2 + m_A u_{0A}^2}{m_A + m_B} = \langle u_0^2 \rangle \\ d &= \frac{\mu^2}{m_A m_B} \end{aligned}\right\} \qquad (62)$$

b and d depend only on the masses involved. C may be called the mean square velocity of the particles A and B. Usually we shall have $a \gg c$.
Equation (61) can be solved for g^2.

$$g_{\pm}^2 = \frac{(b-d)v^2 + (c-a)(b+d) \pm 2v\sqrt{(b+d)(ad+bc) - bdv^2}}{(b+d)^2} \qquad (63)$$

In other words this means that evaluating the integral (59) for a given energy E_c (i.e. for given v) we have to vary g^2 from g_-^2 to g_+^2, with the additional restriction, however, that

$$|u_{oA} - u_{oB}| \leq g \leq u_{oA} + u_{oB} \qquad (64)$$

It proves useful to consider these conditions in the $g^2 - v^2$ plane (figure 1). In this plane equation (61) or (63) is represented by an ellipse with inclined axis. The region from which we get particles is shaded in figure 1. In general the line $g^2 = (u_{oA} + u_{oB})^2$ liesbelow the point A of the ellipse. The values of s for $g = u_{oA} \pm u_{oB}$ are

$$s = \frac{|m_A u_{oA} \pm m_B u_{oB}|}{m_A + m_B} \qquad (65)$$

s may become zero only if $m_A u_{oA} = m_B u_{oB}$, and in this case the line $g^2 = (u_{oA} + u_{oB})^2$ goes through the point A. The inclination of the ellipse depends on the ratio

$$\frac{b}{d} = \frac{(m_A + m_B)m_D}{(m_C + m_D)m_C} \approx \frac{m_D}{m_C} \qquad (66)$$

If $b/d > 1$ it is inclined towards the right, otherwise if $b/d < 1$ it is inclined towards the left. The coordinates of the point B depend on the constants a,b,c,d such that B lies below the v^2-axis if $a \gg c$, which is the case if $Q \gg kT$. This is the situation plotted in figure 1, while figure 2 corresponds to the other case, which is less interesting. As we shall see immediately, the two cases correspond to different types of spectra.

Considering figure 1 we see that there are no particles below and above certain energies corresponding to points R and S of figure 1. Between points T and U the spectrum does not depend on v (or E_c) because the limits of integration do not depend on v in this region and because (as we saw above) the integrand does not depend on v either. The points R,S,T,U thus define the spectrum which is plotted schematically in figure 3. The velocities corresponding to R,S,T,U can be calculated from equation (61) by putting $g^2 = \left(u_{oA} \pm u_{oB}\right)^2$. One finds the total width of the spectrum, expressed in terms of v,

$$\left(\Delta v\right)_{total} = 2\,\frac{m_A u_{oA} + m_B u_{oB}}{m_A + m_B}. \qquad (67)$$

and the width of the plateau

$$\left(\Delta v\right)_{plateau} = 2\,\frac{\left|m_A u_{oA} - m_B u_{oB}\right|}{m_A + m_B} \qquad (68)$$

$\left(\Delta v\right)_{total}$ is twice the maximum value of s and $\left(\Delta v\right)_{plateau}$ is twice its minimum value.
If

$$m_A u_{oA} = m_B u_{oB} \qquad (69)$$

$(\Delta v)_{\text{plateau}}$ disappears, and we get the spectrum of figure 4. Spectra of this type have been computed for the d(d,n) He^3 reaction and can be found in /1/. This spectrum has a peak at

$$\vartheta = \sqrt{v_0^2 + \frac{m_A m_D (m_A+m_B)}{m_B m_C (m_C+m_D)} u_{0A}^2} \approx \sqrt{v_0^2 + \frac{m_A m_D}{m_B m_C} u_{0A}^2} \qquad (70)$$

and the derivatives of the spectrum are finite at this peak.

The derivatives of the spectrum in both cases, figure 3 and figure 4, are zero at R and at S if $u_{0A} = u_{0B}$.

If the point B lies above the ϑ^2-axis as in figure 2, the spectrum may have a somewhat different shape. There are several cases which we could distinguish. In one of the two wings of the spectrum or in both wings there may be an additional singularity, which would cause a discontinuity in the derivative of the spectrum. For the case of figure 2 a spectrum like that of figure 5 would be obtained.

3e. Two-dimensional monoenergetic velocity distributions

For this case

$$\frac{d^2R}{d\Omega dE_c} = \frac{n_A n_B \vartheta}{\pi^3 (b+d) m_c} \int_R \frac{g^2 \sigma(g)\, dg}{\sqrt{a+bg^2}\sqrt{g^2-(u_{0A}-u_{0B})^2}\sqrt{(u_{0A}+u_{0B})^2-g^2}\sqrt{g^2-g_-^2}\sqrt{g_+^2-g^2}} \qquad (71)$$

where (see equations (62))

$$b+d = \frac{\mu}{m_C}\left(\frac{m_D}{m_C+m_D} + \frac{m_C}{m_A+m_B}\right) \approx \frac{\mu}{m_C} \qquad (72)$$

g_+ and g_- are different from the g_+ and g_- of the preceding section, at least in general, because the angle of observation, α, enters the problem (α is the angle between the axis and the direction of observation).

Equation (60) of the preceding section has now to be replaced by

$$v_{\pm} = \sqrt{w_c^2 - s^2\cos^2\alpha} \pm \sqrt{s^2\sin^2\alpha} = \sqrt{A + Bg^2} \pm \sqrt{C - Dg^2} \qquad (73)$$

and equation (63) by

$$g_{\pm}^2 = \frac{(B-D)v^2 + (C-A)(B+D) \pm 2v\sqrt{(B+D)(A+BC) - BDv^2}}{(B+D)^2} \qquad (74)$$

where

$$\begin{aligned} A &= a - c\cos^2\alpha \\ B &= b + d\cos^2\alpha \\ C &= c\sin^2\alpha \\ D &= d\sin^2\alpha \end{aligned} \qquad (75)$$

The problem is thus reduced to the problem treated in the last section if we just replace a,b,c,d by A,B,C,D, which depend on α. Thus, we can obtain the spectra in a very similar manner. We have to take into account, however, the singularities of the integrand in our integral (71). The integrand is singular along all the boundary of the admissible regions of integration and imaginary outside.

The ellipse of figure 6 depends on α and it shrinks if α becomes smaller. It shrinks to a line from D to A for $\alpha = 0$, because in this case

$$v^2 = w_c^2 - s^2 = (a-c) + (b+d)g^2 \qquad (76)$$

i.e. v is a unique function of g in this limit and only pairs of particles with the corresponding relative velocity g contribute to the spectrum at v . The points A and D are fixed, i.e. their position does not depend on α . B and C depend on α in such a way that B moves towards A and C towards D as α tends to zero. This is the shrinking process just mentioned. During this process the point B crosses the v^2-axis and this may cause very strange spectra. If, as we always assume, $a \gg c$ ($Q \gg kT$), B crosses the axis for a very small angle only, which is to the order of magnitude given by

$$\alpha \approx \sqrt{\frac{c}{a}} \tag{77}$$

Thus, the usual situation is that described by figure 6, which allows us to construct the spectrum of figure 7, and which is essentially defined by the properties of the integral (71) at the points R,S,T,U. At each of these points two of the roots in the denominator are zero.

The integral is, however, singular at T and U only, while at R and S the divergence of the integrand is compensated by the fact that the regions of integration also disappear. This is due to the fact that the integral

$$\int_{a^2}^{b^2} \frac{dx^2}{\sqrt{x^2-a^2}\sqrt{b^2-x^2}} = \pi \tag{78}$$

is finite. The spectrum is thus finite at R and S, i.e. it starts and ends with jumps, which are (equation (78) is used to integrate (71))

$$\Delta\left(\frac{d^2R}{d\Omega dE_c}\right) = \frac{n_A n_B v}{2\mu\pi^2} \cdot \frac{g\,\sigma(g)}{\sqrt{a+bg^2}\sqrt{(n_{0A}+n_{0B})^2-g^2}\sqrt{g^2-g_-^2}} \tag{79}$$

where $g^2 = (u_{0A} - u_{0B})^2$ and v is either of the corresponding two values thus obtained from equation (73). g_- is defined by equation (74).

The width of the spectrum and the distance between the two singularities are easily obtained and differ from the three-dimensional results (67) and (68) only by an expected factor $\sin\alpha$.

For $u_{0A} = u_{0B}$ the jumps at R and S are zero and if $m_A u_{0A} = m_B u_{0B}$ the two singularities join into one. For reactions between identical particles both conditions are fulfilled, and we obtain spectra as computed for the d-d reaction in /1/.

Spectra as shown by figure 7 are obtained only for sufficiently large angles α (see (77)). For $\alpha = 0$ the spectrum is schematically given in figure 8. As we have already seen, the ellipse shrinks into a line and along this line $g_- = g_+ = g$, i.e. two roots in the denominator of the integrand are zero. Due to equation (78) the integral does not diverge, however, except for the ends of the spectrum. At these ends a third root is zero (if $u_{0A} \neq u_{0B}$), and the spectrum is divergent (but still, as it has to be, integrable). The width of the spectrum is

$$\Delta v^2 = 4\,(b+d)\,u_{0A}\,u_{0B} \qquad (80)$$

If $u_{0A} = u_{0B}$ one divergence disappears, and one gets the shape of the spectrum given in figure 9.

The transition from large angle spectra (like figure 7) to the $\alpha = 0$ spectrum (figure 8) is rather complicated, and it will not be discussed in detail. Figure 10 gives examples of such intermediate spectra.

Up to now we have facitly assumed that both velocities u_{0A} and u_{0B} are different from zero. If one of them is zero (u_{0B}, for example,) we get spectra of the same type as figure 8 with a width

$$\Delta v = 2 \frac{m_A v_{oA}}{m_A + m_B} \sin\alpha \qquad (81)$$

This may be considered as a special case of figure 7, with the difference, however, that equation (81) is correct for any angle α .

The examples given should be sufficient and other cases can be treated analogously. The strange spectra appearing are, from a practical point of view, not very important anyway. For practical diagnostic purposes only the large angle type of spectrum (figure 7) is of interest.

4. Conclusion

By considering some typical model velocity distributions (Maxwillians and monoenergetic distribution) we have shown that the particles generated by nuclear reactions in energetic plasmas have very typical energy spectra. The measurement of such spectra could be an interesting tool of plasma diagnostics. A very good method would be to add tritium to a deuterium plasma. The d-t reaction has a very large cross section and would produce many neutrons (14 MeV) and α-particles (3.5 MeV), both with a half-width of about 177 $\sqrt{kT}$ keV (for Maxwellian distributions, kT in keV) which should be measurable for high energy plasmas. There is also a very remarkable difference between the almost Gaussian spectrum of Maxwellian plasmas and the spectra of monoenergetic plasmas (as they may be important for the early phases of strong θ-pinches, where one could have two-dimensional monoenergetic distributions). Measurements of the angular dependence of the spectrum and its shape could certainly supply very useful information and could perhaps help to clarify the processes going on in a pinch plasma or in a plasma focus, for instance.

References

/1/ G.Lehner and F.Pohl,
Z.f.Physik 207, (1967) , 83 and Report IPP 1/60 (1967),
English translation: LA-TR-67-113

/2/ C.Andelfinger et al.,
Los Alamos Report LA-3770 (1967) Paper G-2

/3/ C.Andelfinger et al.,
Report IPP 1/67 (1967)

/4/ G. Lehner and F.Pohl,
Report IPP under preparation

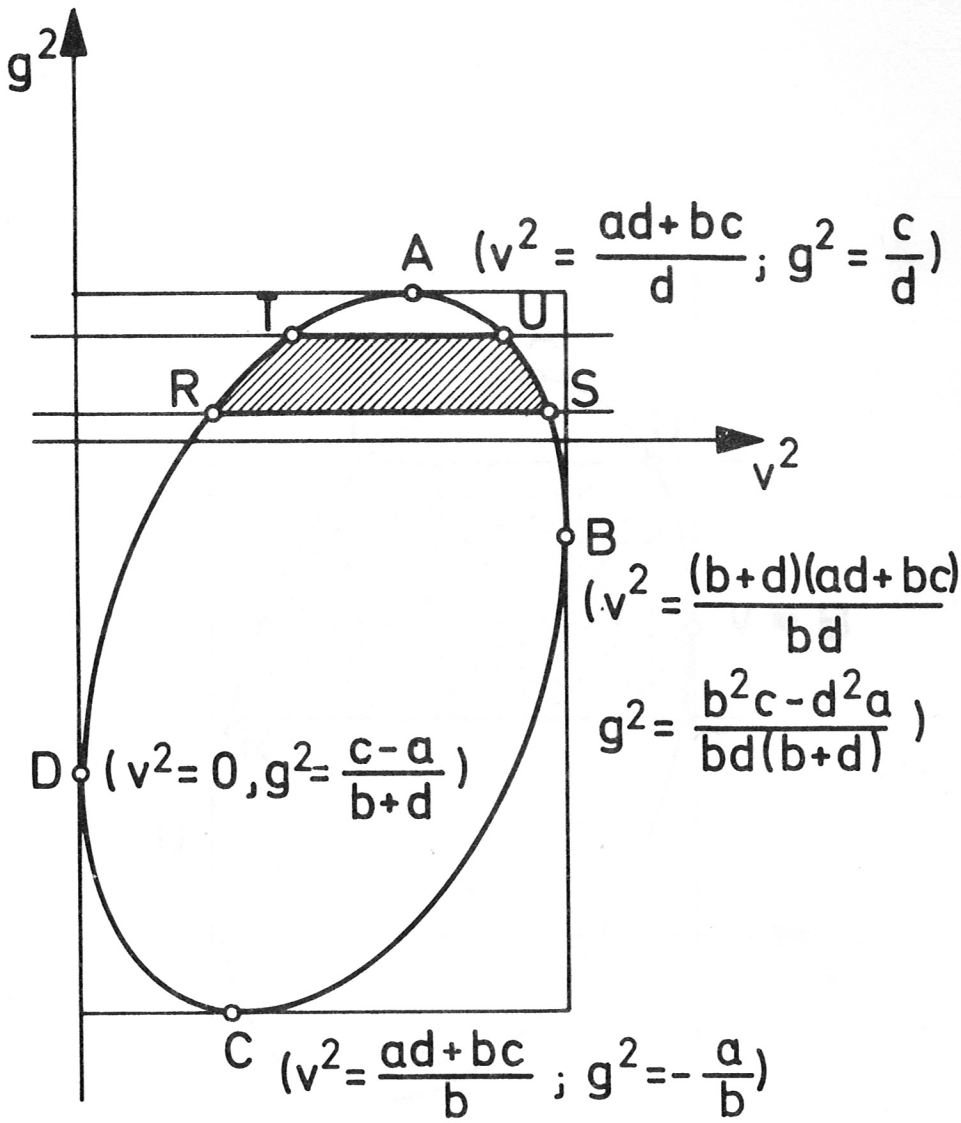

Figure 1 Construction of the spectrum for three-dimensional monoenergetic distributions ($a \gg c$).

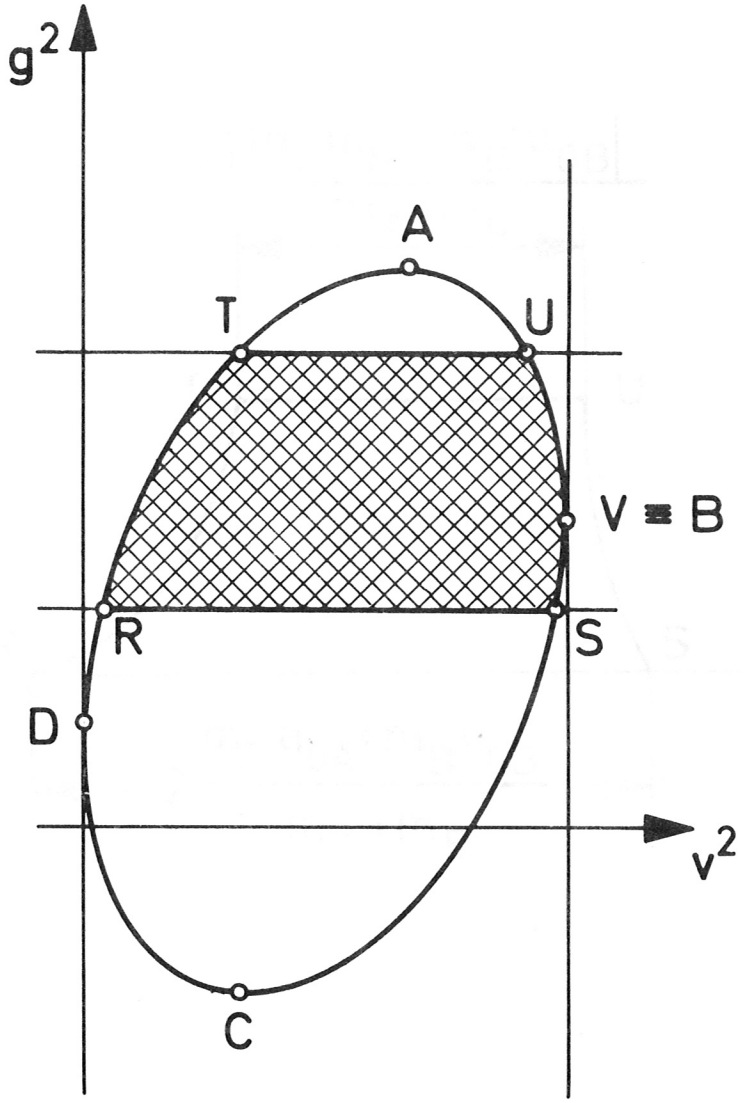

Figure 2 Construction of the spectrum for three-dimensional monoenergetic distributions ($a < c$).

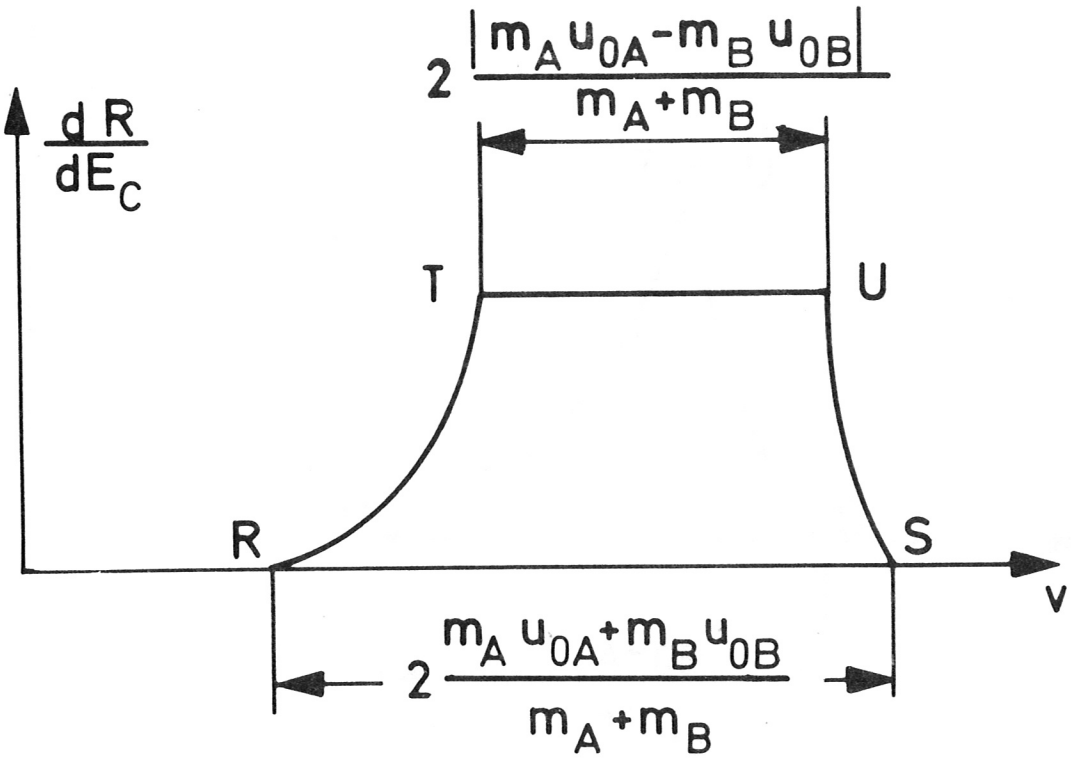

Figure 3 Energy spectrum as a function of v for three-dimensional monoenergetic distributions (schematic) if $m_A u_{0A} \neq m_B u_{0B}$ and $u_{0A} \neq u_{0B}$

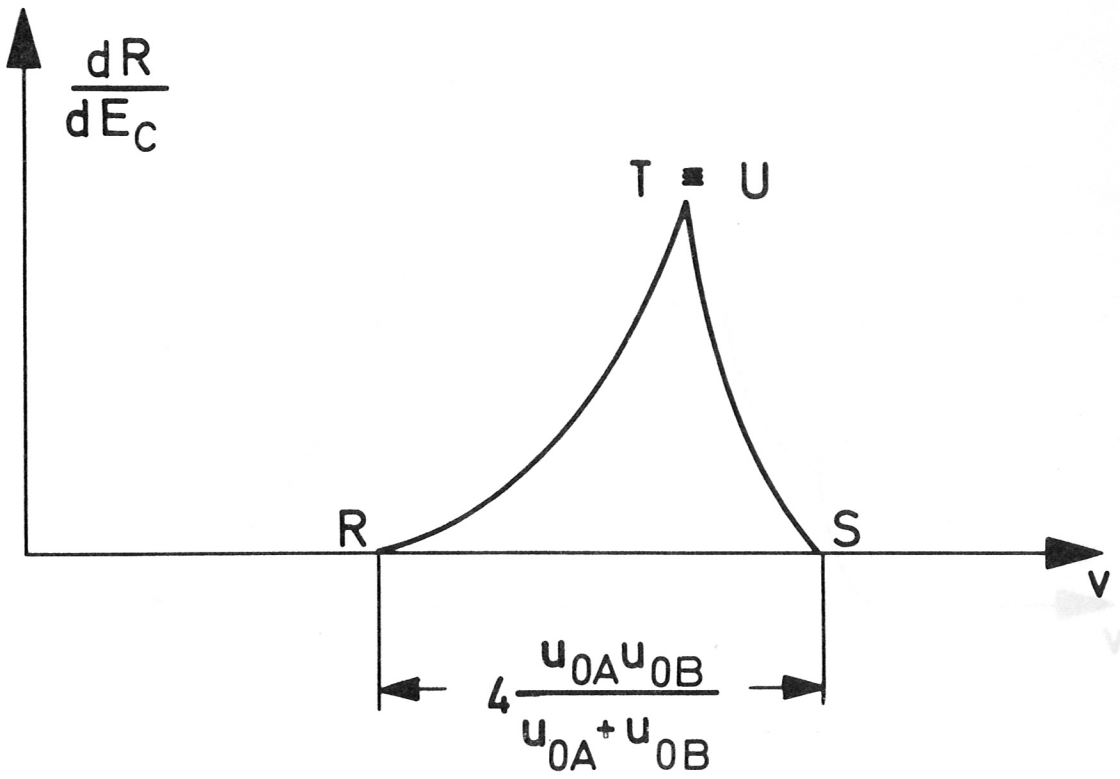

Figure 4 Energy spectrum as a function of for three-dimensional monoenergetic distributions (schematic) if $m_A u_{0A} = m_B u_{0B}$ and $u_{0A} \neq u_{0B}$

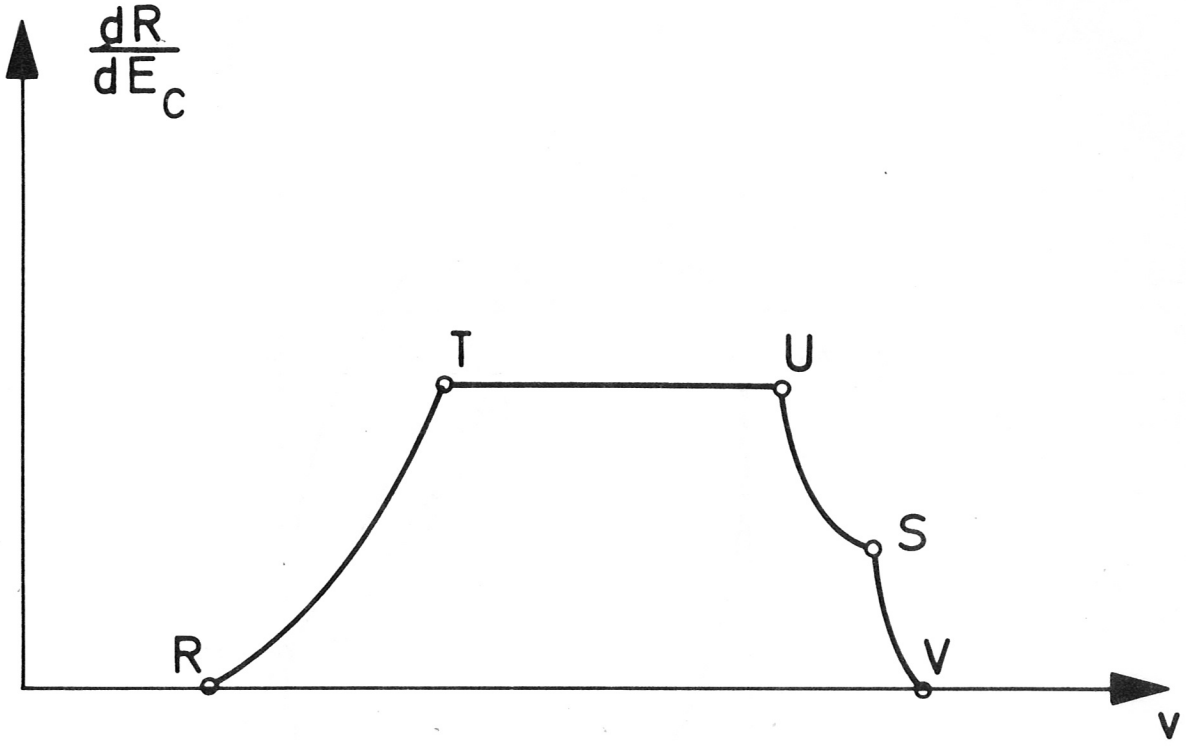

Figure 5 Energy spectrum as a function of ϑ for three-dimensional monoenergetic distributions (schematic) corresponding to the situation described in Fig. 2.

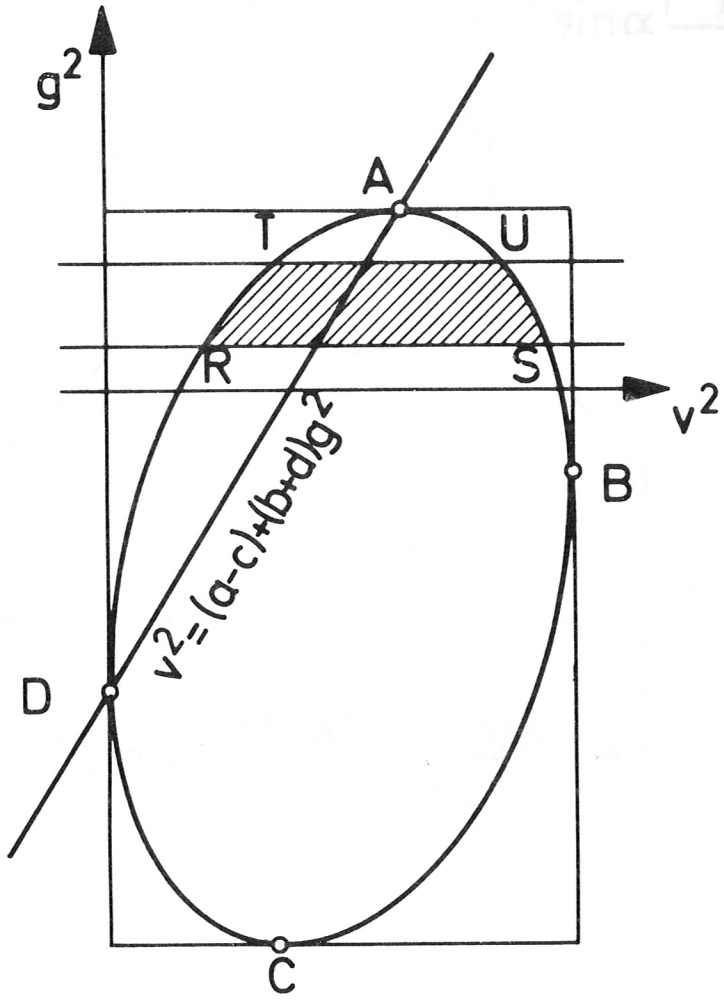

Figure 6 Construction of spectrum for two-dimensional mono-energetic distributions

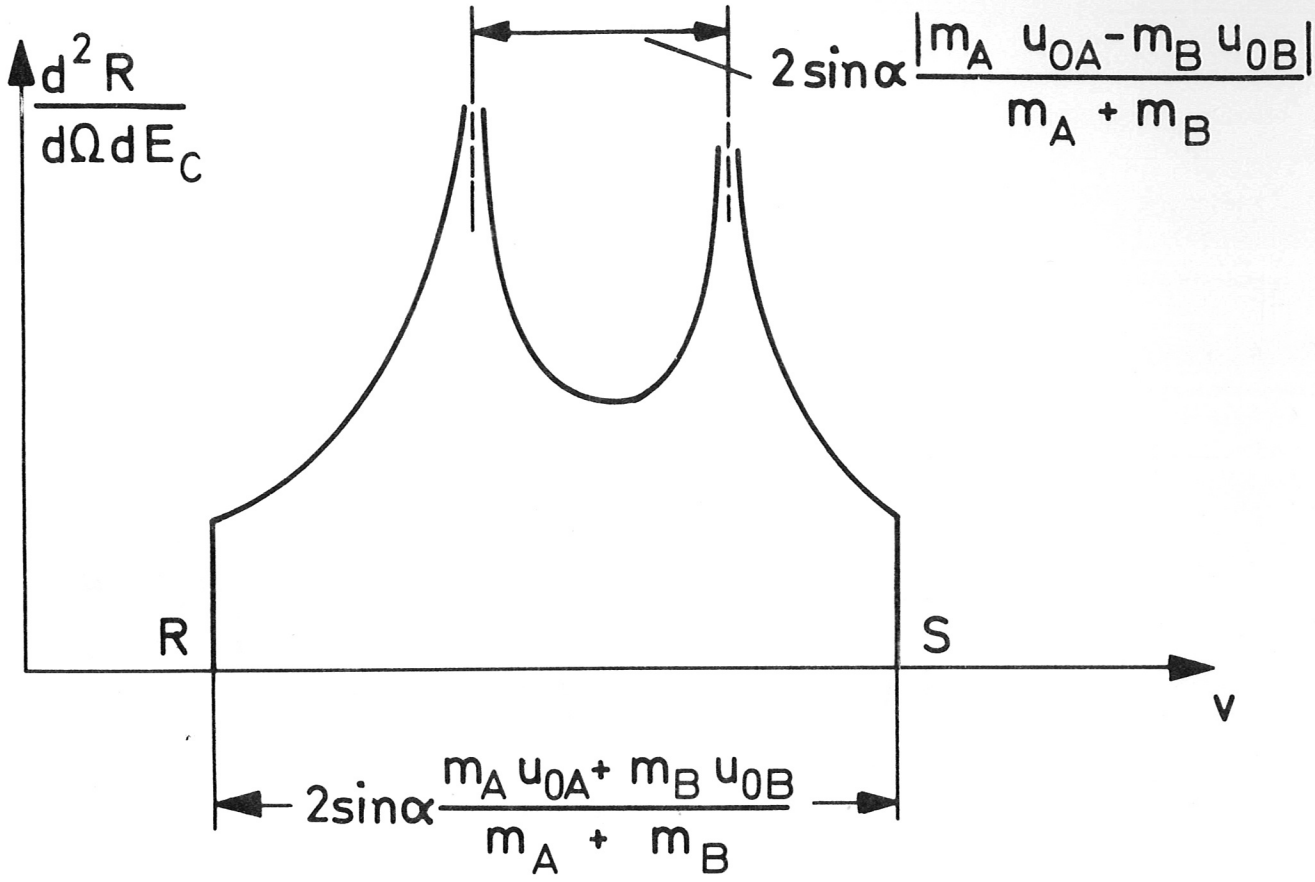

Figure 7 Energy spectrum for two-dimensional monoenergetic distributions and sufficiently large angles α .

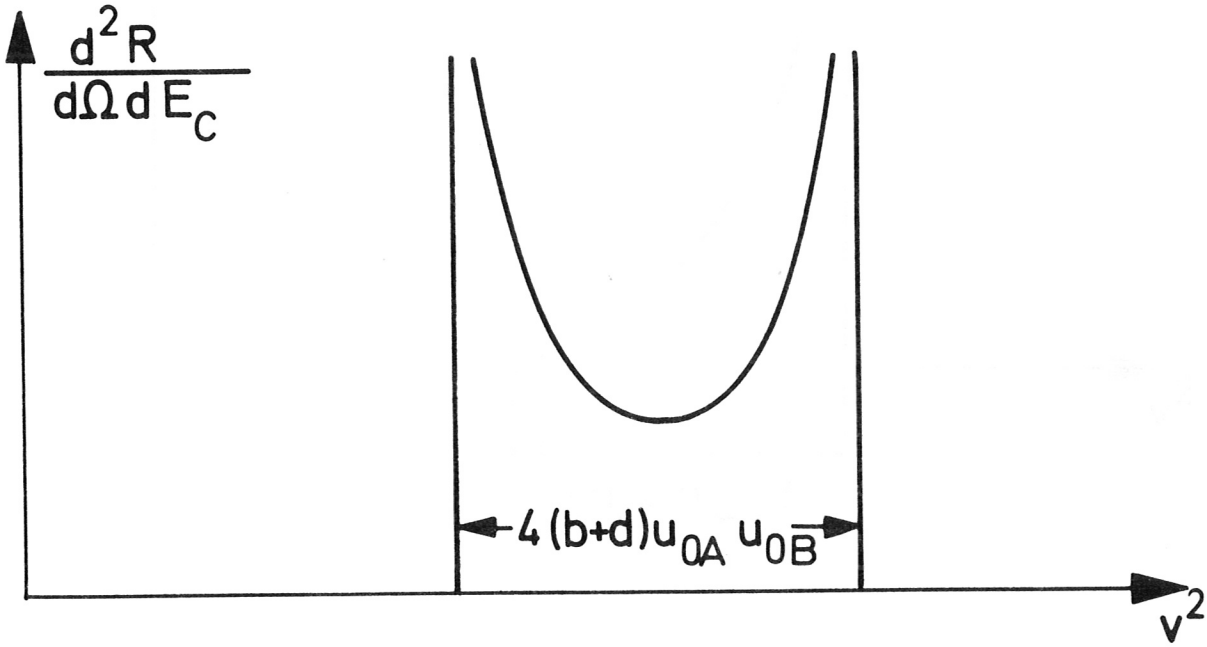

Figure 8 Energy spectrum for two-dimensional monoenergetic distributions at $\alpha = 0$; $u_{0A} \neq u_{0B}$

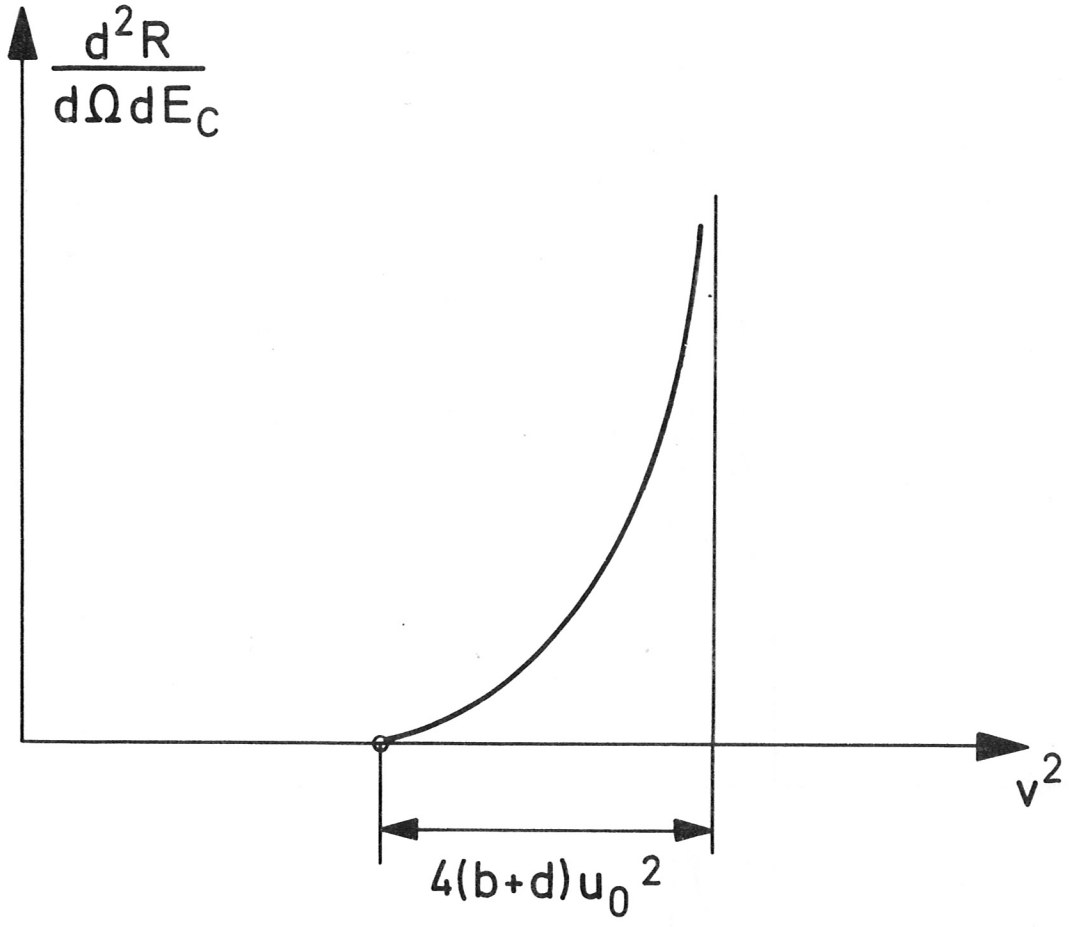

Figure 9 Energy spectrum for two-dimensional monoenergetic distributions at $\alpha = 0$; $u_{0A} = u_{0B} = u_0$; $\Delta v^2 = 4(b+d)u_0^2$.

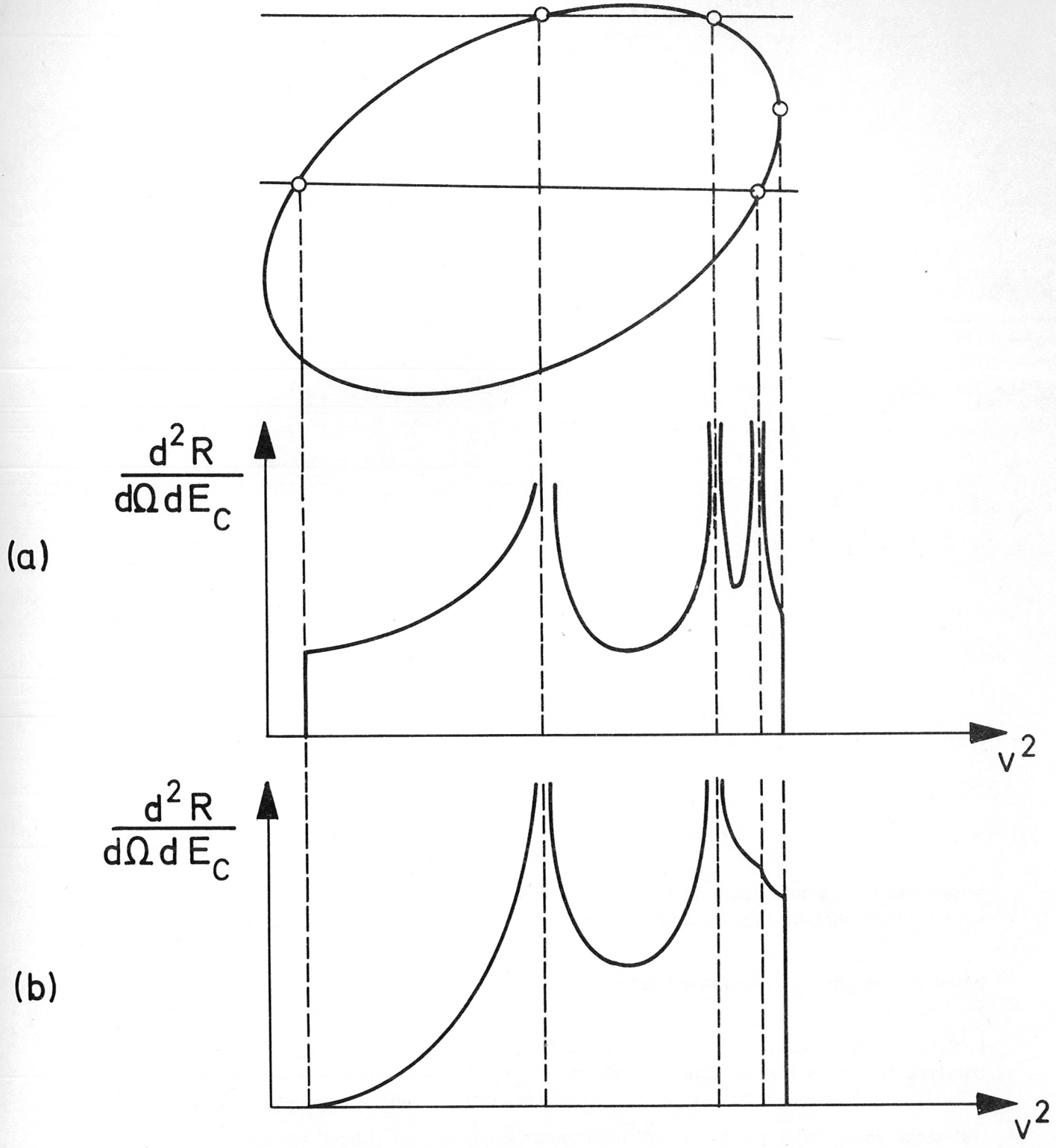

Figure 10 Two examples of spectra for two-dimensional mono-energetic distributions at small angles (a): $u_{0A} \neq u_{0B}$ (b): $u_{0A} = u_{0B}$ In both cases $m_A u_{0A} \neq m_B u_{0B}$.